

From Electron Diffraction to Electron Crystallography

written by Eleni Sarakinou

University of Thessaloniki, Greece, esara@physics.auth.gr

and Julita Smalc-Koziorowska

University of Thessaloniki, Greece, julitasmalc@wp.pl

based on the lecture of Prof. Christos Lioutas

University of Thessaloniki, Greece

1. Diffraction

Diffraction refers to various phenomena associated with the bending of waves when they interact with obstacles in their path. It occurs with any type of wave, including sound waves, water waves, and electromagnetic waves such as visible light, x-rays and radio waves. As physical objects have wave-like properties, diffraction also occurs with matter and can be studied according to the principles of quantum mechanics. While diffraction always occurs when propagating waves encounter obstacles in their paths, its effects are generally most pronounced for waves where the wavelength is on the order of the size of the diffracting objects. The complex patterns resulting from the intensity of a diffracted wave are a result of interference between different parts of a wave that traveled to the observer by different paths.

2. Examples of diffraction in everyday life

The effects of diffraction can be readily seen in everyday life. The most colorful examples of diffraction are those involving light; for example, the closely spaced tracks on a CD or DVD act as a diffraction grating to form the familiar rainbow pattern we see when looking at a disk. This principle can be extended to engineer a grating with a structure such that it will produce any diffraction pattern desired; the hologram on a credit card is an example. Diffraction in the atmosphere by small particles can cause a bright ring to be visible around a bright light source like the sun or the moon. A shadow of a solid object, using light from a compact source, shows small fringes near its edges. All these effects are a consequence of the fact that light is a wave.

Diffraction can occur with any kind of wave. Ocean waves diffract around jetties and other obstacles. Sound waves can diffract around objects, this is the reason we can still hear someone calling us even if we are hiding behind a tree. Diffraction can also be a concern in some technical applications; it sets a fundamental limit to the resolution of a camera, telescope, or microscope.

3. The mechanism of diffraction

Diffraction is the general effect of wave phenomena occurring whenever a portion of a wavefront (elastic, electromagnetic or matter wave) is obstructed in some way. The wavefront is modified from one point to the next one.

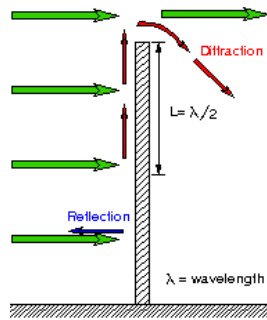


Figure 1: The diffraction phenomenon

The final results on the observed image are :

- The deviation of the intensity distribution that is predicted from the linear propagation
- The increasing or decreasing of the intensity at “unexpected” points that give rise to bright or dark fringes.

4.Huygens – Fresnel principle

The **Huygens–Fresnel principle** (named after Dutch physicist Christiaan Huygens, and French physicist Augustin-Jean Fresnel) is a method of analysis applied to problems of wave propagation (both in the far field limit and in near field diffraction). It recognizes that every unobstructed point of a primary wavefront, at a given instant in time, serves as the source of spherical secondary wavelets that advance with a speed and frequency equal to that of the primary wavefront. Moreover, the primary wavefront at some later time is the envelope of the secondary wavelets.

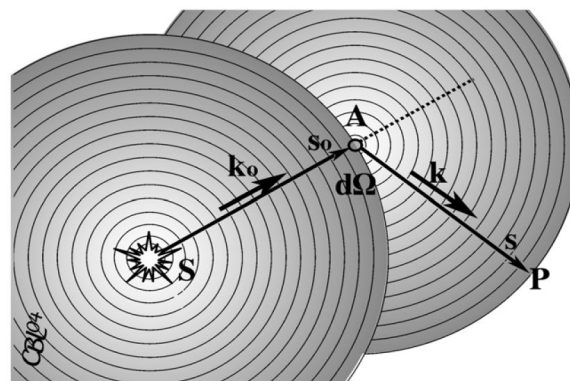


Figure 2: Refraction; Huygens-Fresnel principle

The amplitude of the optical field at a point beyond P is the superposition of all of these waves (considering their amplitudes and relative phases). The calculation requires the integration of the elementary wavelets $d\psi_s$ over all the diffracting space.

5. Electron Diffraction: Basic formula

The optical path – length difference (or the phase difference) must be calculated for every wavelet in relation to an arbitrary origin.

$$\begin{aligned}\Delta\varphi &= \frac{2\pi}{\lambda} (\mathbf{OB} + \mathbf{OC}) = \frac{2\pi}{\lambda} (r\cos\theta_1 + r\cos\theta_2) = 2\pi(\mathbf{k}_0 r\cos\theta_1 + \mathbf{k}_0 r\cos\theta_2) \\ &= 2\pi(-\mathbf{k}_0 \mathbf{r} + \mathbf{k} \mathbf{r}) = 2\pi(-\mathbf{k}_0 + \mathbf{k}) \mathbf{r} = 2\pi \mathbf{K} \mathbf{r}\end{aligned}$$

where, $\frac{1}{\lambda} = |k| = |k_0|$ και $\mathbf{K} = \mathbf{k} - \mathbf{k}_0$

The superposition of the secondary wavelets triple integral over all the diffraction space (Ω) gives the Fourier Transform of the function that describes the potential of the material that induces the electron's diffraction.

$$A(\theta) = \frac{2\pi m_0 e}{h^2} \iiint_{\Omega} V(\mathbf{r}) \exp[i2\pi \mathbf{K} \cdot \mathbf{r}] d\Omega$$

The intensity of every diffracted beam in Fraunhofer diffraction condition is proportional to the Fourier Transform and is observed on the back focal plane of the imaging lens.

The calculations of the diffraction integral in the volume of a unit cell gives as a result the Structural Factor of the diffracted material for a specific diffraction angle θ .

6. The atomic scattering factor $f(\theta)$ for electrons

The atomic form factor, f , is the ratio of the scattering power of an atom by a photon to that of a free electron. Its mathematical equation is :

$$f(\theta) = me^2 \lambda \frac{Z - f_x(\theta)}{2h^2 \sin^2 \theta}$$

where:

θ is the angle between incident – diffracted beam

λ is the electrons wavelength

Z is the atomic number of the element

$f_x(\theta)$ is the X-ray atomic form factor

The calculation of the diffraction integral in the volume of a unit cell gives as a result the Structure Factor of the diffractive material for a specific diffraction angle θ

$$F(\theta) = \sum_j f_j(\theta) \exp[i2\pi \mathbf{K} \cdot \mathbf{r}_j]$$

where:

f_j is the Atomic form factor

$\mathbf{K} = \mathbf{k} - \mathbf{k}_0$

\mathbf{r}_j is the position of the j th atom in the unit cell

7. The perfect crystal

The crystal is a periodic replication of the unit cell, where

$$A(\theta) = \frac{2\pi m_0 e}{h^2} \iiint_{crystal} V(r) \exp[i2\pi(k - k_0) \cdot r] d\Omega \text{ or}$$

$$A(\theta) = F(\theta) \sum_n \exp[i2\pi K r_n]$$

where:

$F(\theta)$ is the Structure Factor

$K = k - k_0$

r_j is the position of the j th atom in the unit cell

8. Bragg's law

A crystalline specimen will diffract the electron beam strongly through well-defined directions (given in angles, q) dependent on electron wavelength and crystal lattice spacing according to Bragg's law,

$$n\lambda_{hkl} = 2d_{hkl} \sin\theta$$

where:

n is an integer

λ is the electron wavelength

d is the crystal lattice spacing between atomic planes

θ is the angle of incidence and also of reflection

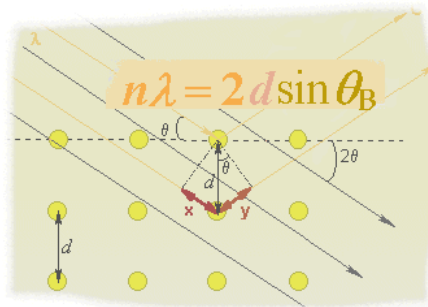


Figure 3: Bragg's Law.

This relation gives the conditions for constructive interference of the scattered electron waves (Fig. 3). There is reinforcement of reflections from successive parallel planes when the angles of incidence and reflection satisfy Bragg's law. The dimensions and spacing of spots are reciprocally related to the lattice dimensions in the specimen. For example, with 100 kV electrons, ($\lambda = 0.0037$ nm) and a d -spacing for a typical biological crystal = 10 nm, $\sin q = 0.000185$ and the Bragg angle $q = 0.0106^\circ$. (A typical d -spacing for a metallic crystal such as nickel is 0.203 nm, so $\sin q = 0.00911$ and $q = 0.522^\circ$).

Depending on the nature of the specimen, a diffraction pattern usually consists of a series of rings (for specimens consisting of many randomly oriented microcrystals) or a discrete lattice of sharp spots (for specimens with a single, crystalline domain). Each sharp spot in the diffraction pattern is an image of the electron source since the imaging system is set to bring the image of the electron source to the viewing screen.

9.Ewald's Sphere

The **Ewald sphere** is a geometric construct used in electron, neutron, and X-ray crystallography which neatly demonstrates the relationship between:

- the wavelength of the incident and diffracted x-ray beams,
- the diffraction angle for a given reflection,
- the reciprocal lattice of the crystal

It was conceived by Paul Peter Ewald, a German physicist and crystallographer.

Ewald's sphere can be used to find the maximum resolution available for a given x-ray wavelength and the unit cell dimensions. It is often simplified to the two-dimensional "Ewald's circle" model or may be referred to as the Ewald sphere.

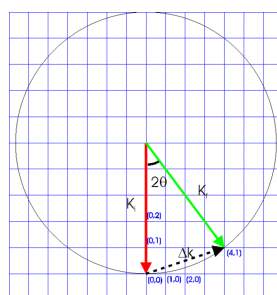


Figure 4: Ewald construction

A crystal can be described as a lattice of points of equal symmetry. The requirement for constructive interference in a diffraction experiment means that in momentum or reciprocal space the values of momentum transfer where constructive interference occurs also form a lattice (the reciprocal lattice). For example, the reciprocal lattice of a simple cubic real-space lattice is also a simple cubic structure. The aim of the Ewald sphere is to determine which lattice planes (represented by the grid points on the reciprocal lattice) will result in a diffracted signal for a given wavelength, λ , of incident radiation.

The incident plane wave falling on the crystal has a wave vector \mathbf{K}_i whose length is $2\pi / \lambda$. The diffracted plane wave has a wave vector \mathbf{K}_f . If no energy is gained or lost in the diffraction process (it is elastic) then \mathbf{K}_f has the same length as \mathbf{K}_i . The amount the beam is diffracted by is defined by the scattering vector $\Delta\mathbf{K} = \mathbf{K}_f - \mathbf{K}_i$. Since \mathbf{K}_i and \mathbf{K}_f have the same length the scattering vector must lie on the surface of a sphere of radius $2\pi / \lambda$. This sphere is called the Ewald sphere.

The reciprocal lattice points are the values of momentum transfer where the Bragg diffraction condition is satisfied and for diffraction to occur the scattering vector must be equal to a reciprocal lattice vector. Geometrically this means that if the origin of reciprocal space is placed at the tip of \mathbf{K}_i then diffraction will occur only for reciprocal lattice points that lie on the surface of the Ewald sphere.

9. Tilting of the specimen

All modern microscopes have specimen holders giving the possibility of the specimen tilting. In a perfect orientation the Ewald's Sphere intersects a plane of the Reciprocal space giving rise to a specific electron diffraction image. With a series of tilting angles successive diffraction images (planes of the reciprocal space) are recorded providing a "full" image of the reciprocal space.

10. Types of electron diffraction patterns

The structure of diffraction patterns depends on the kind of material is under the observation. The main characteristic feature influencing the structure of the diffraction pattern is a level of crystallite. We can resolve:

- **Diffraction pattern of single crystal** (Figure 5) is observed when the diffraction is taken from the sample exhibiting the undisturbed periodic structure over the whole observed area. Then each spot on the diffraction pattern is corresponding to different set of crystallographic planes in the same crystal. The spots are discrete and correspond to the points in reciprocal lattice. Such a diffraction pattern brings the information about the crystallographic structure of investigated material. The angles between diffraction spots are the same as the angles between corresponding directions in the crystal.

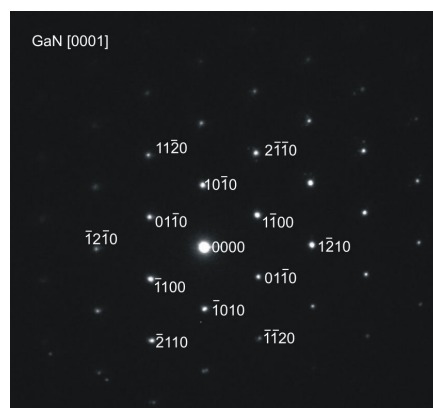


Figure 5. Diffraction pattern taken from single crystal of gallium nitride along 0001 wurtzite zone axis.

- **Diffraction pattern of bi-crystal** (Figure 6) is observed when the diffraction pattern is taken from the area of two discrete structures with specific orientation correlation. Diffraction spots are not in periodic arrangement and correspond to the two independent overlapping diffraction images of single crystals. Such a diffraction pattern brings the information about the relationship between these two crystalline parts of the sample.

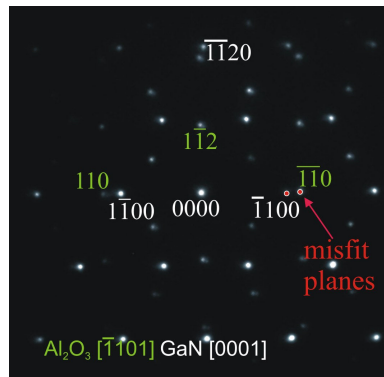


Figure 6. Diffraction pattern taken from bi-crystal of gallium nitride epitaxial film on sapphire substrate. Pattern taken along $[1101]$ sapphire and $[0001]$ gallium nitride zone axes.

- Diffraction pattern of polycrystalline materials** (Figure 7) is observed when the diffraction pattern is taken from the area of a big number of discrete segments with the same structure in random orientations. Diffraction spots are then arranged in concentric rings. The number of spots in every ring depends on the number and size of crystallites. When the spots in the rings are resolvable; the diffraction pattern is taken from a small number of rather large crystallites. In case when the spots in rings are not resolvable it means that the diffraction patterns was taken from a big number of rather small crystallites.

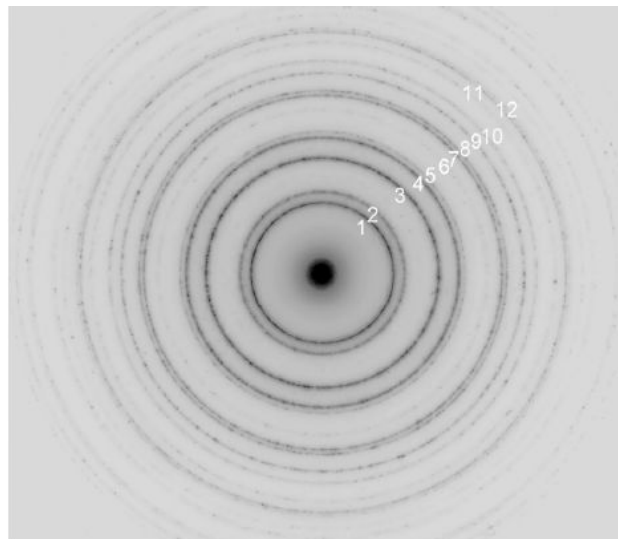


Figure 7. Diffraction pattern taken from polycrystalline gold (inversed contrast).
Courtesy of J.A. Kozubowski

- Diffraction pattern of amorphous material** is observed when the diffraction pattern is taken from area of randomly arranged very small structural units with short range ordering. We can not resolve any discrete spots, and diffraction pattern consists of diffused concentric rings.
- Diffraction pattern of modulated structures** is observed when the diffraction pattern is taken from area of structure with periodic "modification" of basic perfect structure but without any disturbance. In this case we observe a discrete spots coming from single crystal and additional discrete spots with reciprocal lattice vectors perpendicular to the direction of modification.

Distances between additional are inversely proportional to the distances of modification in a real structure.

11. Measurements of electron diffraction patterns

Spots on the diffraction pattern are arranged as points of reciprocal lattice of investigated crystal. It is possible to determine the crystallographic orientation and type of material by the measurements of the spacing between spots and direct beam and measurements of angles between \mathbf{g} vectors.

We can write the Bragg equation: $n\lambda = 2d\sin\theta$

in a different way: $1/2 \cdot 1/d = 1/\lambda \sin\theta$

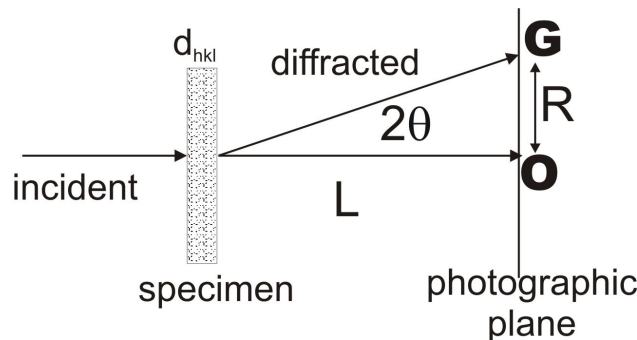


Figure 8. Geometric configuration of electron diffraction on single crystal.

Since in diffraction of fast electrons Bragg angles are very small, about 1° so we can write the proportion:

$$L/Rr = (1/\lambda)(1/d) = d/\lambda$$

And then it is possible to calculate the interplanar spacing for investigated material:

$$d = \lambda L/R$$

where:

λL is a camera constant – characteristic feature of microscope and depends also on magnification of a diffraction pattern

R is a measured on the diffraction pattern the distance between spot coming from direct beam and spot coming from lattice plane (hkl) diffracting the beam. It is a distance OG on figure 8.

12. Structural characterization

Diffraction patterns bring immediately an information about:

- type of material: (mono) crystalline, polycrystalline, amorphous
- complexity: single phase, multiphase, modulation
- faults presence
- cell parameter determination
- symmetry specification (extinction conditions – space group)
- atoms configuration in the unit cell (Creation of artificial diffraction patterns by Fourier transform of simulated structures and comparison results with real diffraction pattern)

13. Case studies

13.1 Phase distinction in the catalytic system TiO₂-Ru

Rutile is the most common natural form of TiO₂. Two rarer polymorphs of TiO₂ are known: anatase (sometimes known by the obsolete name 'octahedrite'), a tetragonal mineral of pseudo-octahedral habit; and brookite, an orthorhombic mineral.

Rutile has among the highest refractive indices of any known mineral and also exhibits high dispersion. Natural rutile may contain up to 10% iron and significant amounts of niobium and tantalum. Rutile is a common accessory mineral in high-temperature and high-pressure metamorphic rocks and in igneous rocks. Rutile is the preferred polymorph of TiO₂ in such environments because it has the lowest molecular volume of the three polymorphs; it is thus the primary titanium bearing phase in most high pressure metamorphic rocks, chiefly eclogites. Brookite and anatase are typical polymorphs of rutile formed by retrogression of metamorphic rutile. Rutile has a tetragonal unit cell, with unit cell parameters $a=4.584\text{\AA}$, and $c=2.953\text{\AA}$

Anatase is always found as small, isolated and sharply developed crystals, and like rutile, a more commonly occurring modification of titanium dioxide, it crystallizes in the tetragonal system; but, although the degree of symmetry is the same for both, there is no relation between the interfacial angles of the two minerals, except, of course, in the prism-zone of 45° and 90°. The common pyramid of anatase, parallel to the faces of which there are perfect cleavages, has an angle over the polar edge of 82°9', the corresponding angle of rutile being 56°52½'. It was on account of this steeper pyramid of anatase that the mineral was named, by RJ Haüy in 1801, from the Greek *anataxis*, "extension," the vertical axis of the crystals being longer than in rutile. There are also important differences between the physical characters of anatase and rutile; the former is not quite so hard ($H=5\frac{1}{2}$ –6) or dense (specific gravity 3.9); it is optically negative, rutile being positive; and its lustre is even more strongly adamantine or metallic-adamantine than that of rutile.

Titanium dioxide is an important material for a variety of applications such as catalytic devices, solar cells, and other optoelectronic devices. The properties of titanium dioxide, especially the catalytic properties, have proved to be strongly related to its crystal structure and grain size. Titanium dioxide in the anatase phase appears to be the most active species for most substrates. Nanocrystalline titanium dioxide undergoes phase transformation and grain growth at relatively lower temperatures, which limits its applications in many fields such as high temperature gas separation and membrane reactors. This high thermal stability of the membranes allows it to be used for gas separation at high temperatures, especially in combination with a chemical reaction where the membrane is used as a catalyst as well as a selective barrier to remove one of the components which has been formed. In order to improve the thermal and physical properties of titania fibers, the doped titania composite membranes were prepared. Solar energy is believed to be an essential energy source of the next century. A pn type solar cell with all solid-state TiO₂ based materials seems to have many benefits for effective utilization of the solar energy because the ultra violet and visible light of solar light would be adsorbed by n-type TiO₂ and p-type TiO₂, respectively. Here, transparent semiconductor electrodes with high conductivity are required. Transparent semiconductive n-type TiO₂ materials were prepared by codoping ruthenium.

Dye-sensitized solar cells (DSSCs) based on nanocrystalline titanium dioxide (TiO₂) thin films have received much research attention in the past decade. These solar cells have reported solar-to-electric energy conversion efficiencies of greater than 10%. Given the low cost of their components and their demonstrated conversion

efficiencies, DSSCs show true promise for being an inexpensive, renewable, and environmentally benign alternative to fossil fuels. DSSCs are made by covalently bonding a sensitizer dye to the surface of a thin film of nanocrystalline TiO_2 , which does not absorb visible light because it is a wide-gap semiconductor. Sensitization with a dye, such as Ruthenium-535 [$\text{Ru}(4,4'\text{-dicarboxy-2,2'\text{-bipyridine})}_2(\text{NCS})_2$], greatly enhances the ability of these cells to absorb sunlight. Electrons are injected from the dye molecule's excited state to the conduction band of the TiO_2 on a sub-picosecond time scale, where they are conducted through the electrical circuit (shown on Fig. 9).

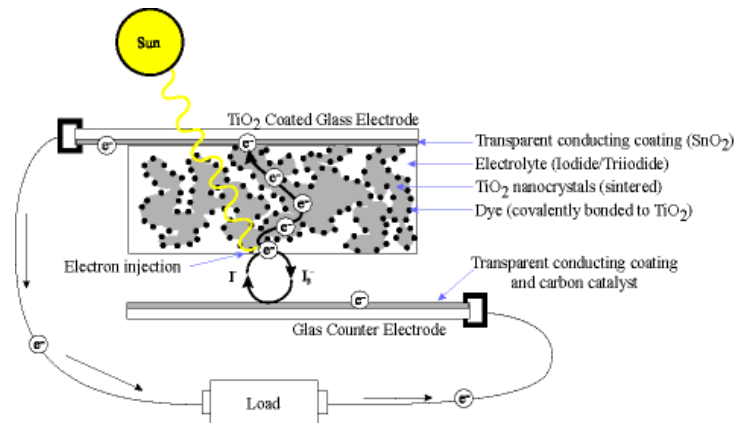


Figure 9. Schematic representation of solar cell.

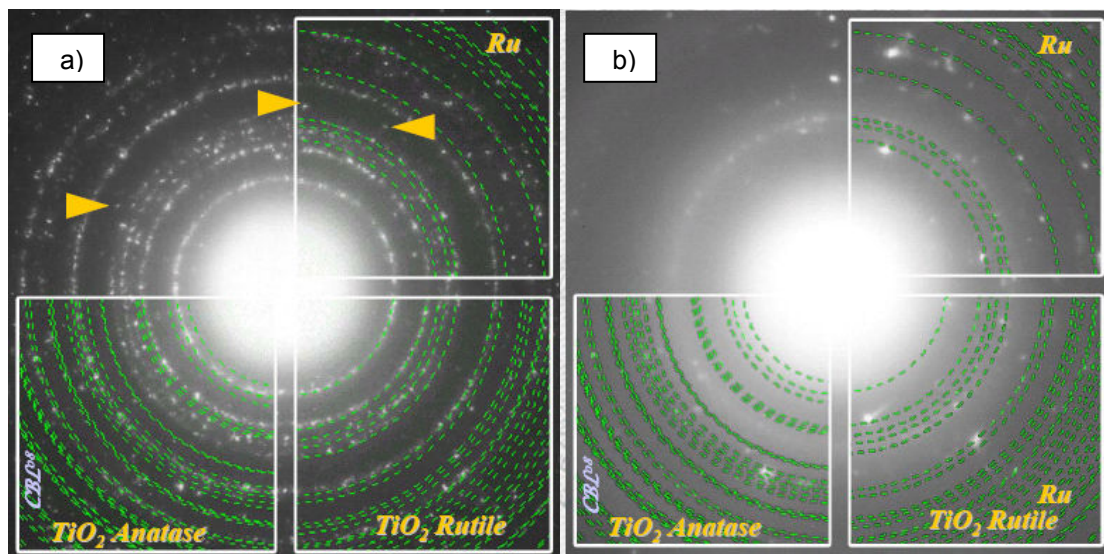


Figure 10. Diffraction patterns of a) the polycrystalline matrix material, b) crystallinities .

In this case study, the polycrystalline complex of $\text{TiO}_2\text{-Ru}$ was investigated. The diffraction pattern shown on Fig 10a) was taken from matrix material and it consists of concentric rings. The diffraction rings are composed of discrete spots what indicates that the matrix material consists of small number of rather large crystallites. To find the material of the matrix the ring diffraction pattern for rutile form and anatase form of titanium dioxide and for ruthenium crystals were prepared and then compared with the real diffraction pattern. It is visible that the simulated rings of rutile match very well with the rings visible on the diffraction pattern and this is also the main phase of matrix material. Some discrete spots between rutile rings (yellow arrows) cover with simulated diffraction rings of anatase phase, this indicate for the rare appearance of the anatase crystallites

in matrix material. The simulated spots for Ru are situated very close to that of TiO_2 , but Ru is not observed in matrix material. The diffraction pattern shown on Fig 10b) was taken from area with bigger crystals and its analysis indicates that bigger crystals are TiO_2 rutile crystals (discrete spots are observed). It is also visible that weak spots are coming from ruthenium small crystallites.

13.2 Structural characterization of $\text{Al}_x\text{Ga}_{1-x}\text{N}$ films grown on sapphire

Gallium nitride and its alloys with aluminium and indium are the group of semiconductors which are widely used in many optoelectronic applications. AlGaN is used to manufacture light-emitting diodes operating in blue to ultraviolet region, where wavelengths down to 250 nm (far UV) were achieved. It is also used in blue semiconductor lasers, detectors of ultraviolet radiation, and in AlGaN/GaN HEMT transistors. Nitrides are very hard, mechanically stable materials with large heat capacity. GaN in its pure form it resists cracking and can be deposited in thin film on sapphire or silicon carbide, despite the mismatch in their lattice constants. GaN can be doped with silicon (Si) or with oxygen to N-type and with magnesium (Mg) to P-type, however the Si and Mg atoms change the way the GaN crystals grow, introducing tensile stresses and making them brittle. Gallium nitride compounds also tend to have a high spatial defect frequency, on the order of a hundred million to ten billion defects per square centimeter.

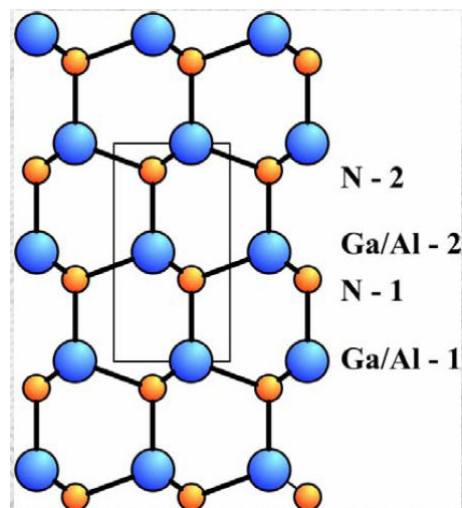


Figure 11. Schematic representation of AlGaN wurtzite structure.

In this case studies it was shown that the percentage composition of Al in AlGaN alloy can be determined with diffraction pattern analysis. AlGaN may crystallize in wurtzite structure with crystallographic symmetry group $P6_3mc(186)$. The lattice constants of pure wurtzite GaN are $c=0.519$ nm and $a= 0.359$ and these values are diminished since aluminium atom is much smaller than the gallium atoms and their values depend on aluminium composition in AlGaN.

According to the rule for structure factor, some reflections should not appear in case of pure GaN, and forbidden reflection for:

$[1\bar{1}_0]$ zone axis are: $g00.1$, $g00.3$, $g30.1$ and $g 30.3$

$[01\bar{0}]$ zone axis are: $g00.1$, $g00.3$, $g11.1$ and $g11.3$

However for AlGaN this rule is not true and these reflections would be visible when some order in AlGaN occurs.

In Table 1 the different possible composition of alternative 00.1 planes in AlGaN are listed. Positions 1 and 2 respond to two possible positions in a crystallographic cell of wurtzite structure.

Table 1. Interplay between occupation of Ga-Al sites in alternative (00.1) planes

Atom	GaN	AlN	AlGaN-I	AlGaN-II	AlGaN-III	AlGaN-IV
Ga-1	1.0	0.0	0.5	0.7	1.0	1.0
Ga-2	1.0	0.0	0.5	0.3	0.0	0.1
Al-1	0.0	1.0	0.5	0.3	0.0	0.0
Al-2	0.0	1.0	0.5	0.7	1.0	0.9

Intensity of forbidden reflection may be calculated for each possible configuration of (00.1) planes in AlGaN structure (values listed in Table 2) and the calculated values could be compared with intensities of the forbidden reflections measured on the diffraction patterns. In this way the modulation in occupancy of Al-Ga atoms in (00.1) planes could be determined.

Table2. Calculated intensities for different modulations:zone axis [010]

H	K	L	Dhkl	Rhkl	GaN	AlN	AlGaN-I	AlGaN-II	AlGaN-III	AlGaN-IV
0	0	1	5.113	5.68	0.0	0.0	0.0	0.625	3.9	3.05
3	0	1	0.9	32.15	0.0	0.0	0.0	0.1767	1.10	0.86
0	0	3	1.7	17.03	0.0	0.0	0.0	0.49	3.11	2.43
3	0	3	0.81	35.95	0.0	0.0	0.0	0.137	0.858	0.671

The intensities of the forbidden reflections measured on the diffraction patterns could be different than the calculated values – since the dynamical scattering of electrons always occurs and changes the intensity of reflections.

14. References

- [1] <http://en.wikipedia.org/wiki/Diffraction>
- [2] D.B. Williams, C.B. Carter, "Transmission Electron Microscopy- A textbook for materials science" – second part "Diffraction". Plenum Press, New York 1996